

Intraorbital optic nerve stimulation with penetrating electrodes: in vivo electrophysiology study in rabbits

Liming Li · Pengjia Cao · Mingjie Sun · Xinyu Chai ·
Kaijie Wu · Xun Xu · Xiaoxin Li · Qiushi Ren

Received: 4 January 2008 / Revised: 26 August 2008 / Accepted: 6 October 2008 / Published online: 7 November 2008
© Springer-Verlag 2008

Abstract

Purpose To investigate the response properties of the electrically evoked potentials (EEPs) elicited by intraorbital optic nerve stimulation with penetrating electrodes using different stimulus parameters.

Methods Visually evoked potentials (VEPs) were recorded as a control and for comparative purposes. Teflon-coated tungsten wire electrodes (100 μm core-diameter, 300 μm exposed tip) were inserted intraorbitally into the optic nerve. A charge-balanced biphasic current was delivered to the optic nerve via inserted wire electrodes in 26 anaesthetized rabbits. EEPs were recorded by epidural electrodes

placed over the visual cortex. The charge density threshold for eliciting EEPs was determined. Stimulus pulse amplitude, duration, frequency and waveform were varied to study their effects on EEPs. After the experiments, the stimulated optic nerves were examined histologically for examination of implantation position of the stimulating electrode into the optic nerve tissue.

Results EEPs were successfully elicited by intraorbital optic nerve stimulation with penetrating electrodes. The measured amplitude of the first large positive peak (P1) was smaller and the latency of P1 was shorter compared with VEPs. The measured charge density threshold to elicit EEPs was $21.36 \pm 5.64 \mu\text{C}/\text{cm}^2$. The amplitude of P1 increased and the latency of P1 decreased with increasing pulse amplitude of fixed duration stimuli. The amplitude of P1 increased with increasing pulse duration of fixed amplitude stimuli. For fixed charge stimuli, the amplitude of P1 decreased and the latency of P1 increased as the pulse duration increased. As frequency of stimuli varied from 1 to 10 Hz, the amplitude of P1 decreased monotonically. Among the different charge-balanced biphasic pulse stimulating waveforms, the symmetrical cathode-first biphasic pulse elicited the largest amplitude of P1.

Conclusions Our study demonstrates that intraorbital optic nerve stimulation with different stimulus parameters by penetrating electrodes can evoke cortical responses with different properties. The short-duration symmetrical cathode-first biphasic pulses of current with low frequencies are more efficacious in eliciting electrophysiological responses in the visual cortex than other stimulating waveforms.

This research is supported by the National Basic Research Program of China (973 Program, 2005CB724302), National Science Fund for Distinguished Young Scholars from The National Natural Science Foundation of China (60588101), Shanghai Pujiang Program (07pj14050), Shanghai Commission of Science and Technology (05DZ22318, 05DZ22325, 04DZ05114).

L. Li · P. Cao · M. Sun · X. Chai · K. Wu · Q. Ren (✉)
Institute for Laser Medicine and Bio-Photonics,
Department of Biomedical Engineering,
Shanghai Jiao Tong University,
Room 423, Life-Science Building 2,
800 Dong-Chuan Road,
Shanghai 200240, China
e-mail: renqsh@sjtu.edu.cn

X. Xu
Department of Ophthalmology,
Shanghai Jiao Tong University
Affiliated Shanghai First People's Hospital,
Shanghai 200080, China

X. Li
Department of Ophthalmology,
Beijing University
Affiliated Beijing People's Hospital,
Beijing 100044, China

Keywords Visual prosthesis · Optic nerve ·
Electrophysiology · Penetrating electrodes ·
EEPs (electrically evoked potentials) ·
VEPs (visually evoked potentials)

Introduction

Retinal diseases, such as retinitis pigmentosa (RP) or age-related macular degeneration (AMD), are leading causes of untreatable blindness [12, 23]. Micro-electronic based visual prostheses hold great promise for the treatment of such diseases [26]. Since a large percentage of the inner retinal neurons remain intact in patients with RP or AMD [16, 21, 22, 39], many research efforts have been made to develop retinal stimulation based visual prostheses [3, 6, 7, 14, 20, 24, 25, 32, 33, 37, 43–52]. Some preliminary clinical success has been reported by several groups [4, 13, 15, 34, 35].

Another alternative for visual prosthesis is based on optic nerve stimulation. The optic nerve contains approximately 1 million axons of ganglion cells packed into a 2 mm diameter cylinder space in humans, where the whole visual area is represented in a relatively small space. Electrical stimulation of the optic nerve could possibly cover the entire visual field [26]. Veraart and his associates have reported that phosphenes were induced in a blind volunteer by implanting a four-contact self-sizing surface spiral cuff electrode around the optic nerve for electrical stimulation [41]. The patient was reported as being able to recognize simple patterns and discriminate orientation after encoded electrical stimulation was applied to her optic nerve [42].

Neural microstimulation with penetrating electrodes has been reported to have a low threshold and provide a high resolution compared with surface electrodes [1, 2, 36]. Therefore, our group has proposed a novel visual prosthesis based on intraorbital optic nerve stimulation with penetrating electrodes recently [30]. In our approach, the penetrating multi-electrode array is inserted into the optic nerve as a neural interface to couple the encoded electro-stimuli into the axons of the ganglion cells for vision recovery. The optic nerve is chosen as the stimulating site because it is relatively spared by the most prevalent degenerative eye diseases, and can be accessed intraorbitally via a comparably easy surgical procedure without disturbing the already diseased retinal tissues. By selecting a penetrating electrode array, the axons of the ganglion cells local to each electrode could be stimulated. This local approach may potentially increase the spatial resolution of the visual prosthesis while lowering the thresholds of the stimulating current when compared with surface cuff electrodes.

Many studies have been carried out to investigate the response properties elicited by extracellular electrical stimulation of the retina with different parameters [18, 24, 31, 34]. However, the response properties may vary as different neural tissues are electrically stimulated. To develop an appropriate visual prosthesis based on intraorbital optic nerve stimulation, the optimal stimulus

parameters, including pulse amplitude, duration, charge, frequency and waveform, need to be defined. In this study, we investigated the feasibility of the intraorbital optic nerve stimulation with penetrating electrodes in rabbits, and studied the effects of varying stimulus parameters on the response properties of the electrically evoked potentials (EEPs) systematically. The results obtained in the study will provide direct experimental data for designing an optimal visual prosthesis based on intraorbital optic nerve stimulation with penetrating electrodes.

Materials and methods

Subjects

All experimental methods and animal care procedures complied with the ARVO Statement for the Use of Animals in Ophthalmic and Vision Research and the policies in the Guide to the Care and Use of Laboratory Animals issued by the NIH. Twenty-six albino rabbits (Fengxian, Shanghai, China), weighing 2.5–3.0 kg, were used in the experiments.

Surgical procedures

Anesthesia was achieved by intravenous injection of pentobarbital sodium (Pentobarbital sodium, Urchem Ltd, Shanghai, China) with the dose level of 5 mg/kg for induction, and maintained with the dose of 15 mg/kg/h. Electrocardiograph (ECG) and respiration rate were monitored by a multi-channel physiological signal analyzer (MPA 2000, ALCBIO Ltd., Shanghai, China), and body temperature was measured and maintained at 39.8°C by a temperature controller (Model: H-KWDY-III, Xinxiaoyuan Biotech Ltd., Nanjing, China) throughout the experiment. An ophthalmic surgical microscope (SM-2000L, EDER Medical Equipment Ltd., Shanghai, China) with motorized focus and magnification control was used for surgical manipulation. The right eye of each rabbit was used for photic and electrical stimulation in this study. After shaving the area between the upper eyelid and the midline of the skull, the rabbit was fixed in the stereotactic frame (Model for rabbit & cat, ALCBIO Ltd., Shanghai, China).

Before the exposure of the optic nerve, two drops of a mixture of tropicamide (Tropicamide-DCPC, Double Cranes Pharmaceutical Co., Ltd., Beijing, China) and neosynephrine (Adrenaline Hydrochloride Injection, Harvest Pharmaceutical Co., Ltd., Shanghai, China) were used to dilate the pupil and shrink the conjunctiva. An arch incision on the skin was made approximately 3 mm above the upper eyelid. Both the orbicularis oculi muscle and levator muscle were separated from the fascia and retracted to expose the cartilage of the upper orbit. An incision was made

between the cartilage and the frontal bone, and the opening was enlarged along the bony edge to 14 mm until the periorbital was seen clearly. The orbital fascia was opened carefully until the superior rectus muscle was seen, and then the superior rectus muscle at its insertion was cut and retracted. The optic nerve, about 2 mm in diameter, was exposed clearly with slight retraction of the eyeball for the insertion of the stimulating electrode.

In order to detect the maximal response of EEPs, a nine-recording-electrode array was placed over the visual cortex area (Fig. 1). The skull was exposed through a skin incision at the top of the head along the midline, and nine holes were drilled by a micro bone drill (Micro Motor Handpiece Strong 230, Saeshin Precision Ind. Co., Daegu, Korea) over the visual cortex contralateral to the stimulated eye. The nine holes formed a 3×3 array with 2 mm spacing. The center hole was 7 mm anterior to the lambdoid suture and 6 mm lateral to the midline. Nine screw-type stainless steel electrodes (diameter=800 μm) were screwed into the nine holes respectively to contact the dura mater, and were used for recording the cortical responses. As a reference electrode, a screw-type stainless steel electrode was screwed into the hole which was drilled 6 mm anterior to the bregma suture and 4 mm lateral to the midline

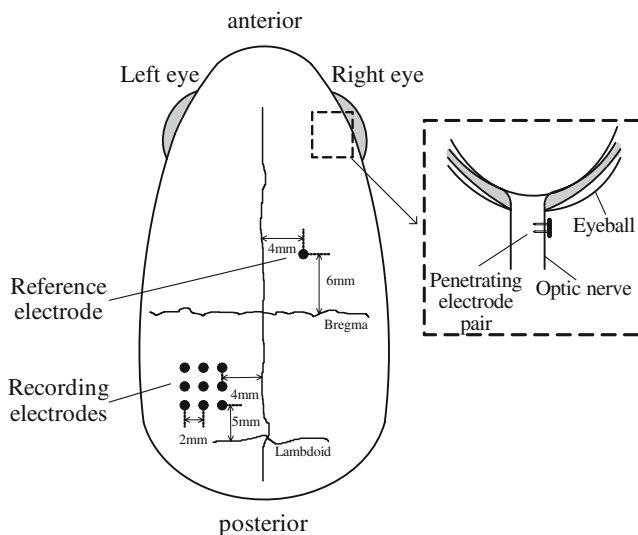


Fig. 1 Schematic diagram of anatomical position for intraorbital optic nerve stimulation and epidural recordings. The right eye was used for electrical stimulation. The stimulating electrode pair with spacing of 1 mm was inserted into the optic nerve intraorbitally, about 1 mm behind the eyeball. The stimulating electrode was anterior to the return electrode, relative to the eyeball. The nine epidural recording electrodes (left, black circles) were placed contralateral to the stimulated eye, forming a 3×3 array with 2 mm spacing. The center recording electrode was placed 7 mm anterior to the lambdoid suture and 6 mm lateral to the midline. The epidural reference electrode (right, black circle) was placed 6 mm anterior to the bregma suture and 4 mm lateral to the midline, ipsilateral to the stimulated eye

contralateral to the recording electrodes. A needle-type stainless steel electrode was placed subcutaneously in the earlobe as the ground electrode.

Photic and electrical stimulations

As a control and for comparative purposes, we recorded white-light bright-flash full-field visually evoked potentials (VEPs) during the entire experiment. The light source, a photic stimulator (LS1130, Tucker-Davis Technologies, Alachua, FL, USA), was positioned 2 cm in front of the right eye. The flash power of the photic stimulator was 90 mJ with an interval of 1 second.

For electrical stimulation of the optic nerve, the electrodes were inserted into the optic nerve via the intraorbital surgical opening. Each electrode was made of Teflon-insulated tungsten wire with 100 μm core-diameter. The front-end of the stimulating electrode was chemically etched to form a sharp tip with a 300 μm exposure after removal of the insulating layer (Fig. 2). The impedance of the electrode was measured in saline by using a Precision LCR meter (E4980A, Agilent Technologies, Santa Clara, CA, USA) with measured values ranging from 2.5–3.5 kΩ at 1 kHz, 50 mV sinusoidal wave. The stimulating and return electrodes were embedded in an epoxy resin substrate to form an electrode pair. Center-to-center spacing of the electrodes was 1 mm. Under the surgical microscope, the stimulating electrode pair was penetrated through the dura, arachnoid and pia mater and carefully inserted, using ophthalmic forceps, into the optic nerve along its axis. The insertion site of the stimulating and return electrodes was about 1 mm and 2 mm respectively, posterior to the eyeball (Fig. 1).

A single charge-balanced biphasic pulse of current (Fig. 3a), generated by an isolated and programmable current source stimulator (MS16, Tucker-Davis Technologies, Alachua, FL, USA), was applied between the stimulating and return electrodes. Pulse amplitude, duration, frequency and waveform of the current stimuli were varied to study their effects on EEPs. The effects of stimulus pulse amplitude on EEPs were investigated by using current intensity ranging from 40 to 120 μA with a fixed pulse duration of 0.5 ms. The effects of stimulus pulse duration on EEPs were studied over a range of 0.4 to 1.2 ms with a fixed pulse amplitude of 100 μA. By holding the charge constant, the effects of varying pulse duration and correspondingly varying pulse amplitude on EEPs were examined. For the above experiments, charge-balanced symmetrical cathode-first biphasic pulses (Fig. 3a) were used at a frequency of 1 Hz.

For evaluating the effects of stimulus frequency on EEPs, the same waveform as above was used, and the frequency of the stimuli was varied from 1 to 10 Hz.

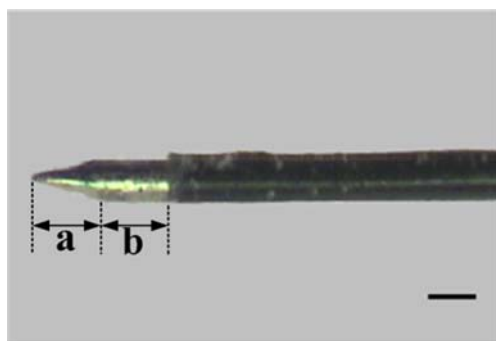


Fig. 2 Penetrating electrode. Teflon-coated tungsten wire, 100 μm core-diameter, 300 μm -length exposed tip with a 150 μm cone head (a) and a 150 μm shaft (b). Scale bar: 100 μm

To investigate the effects of stimulus waveform, five different charge-balanced patterns were applied. The total charge of each of these five patterns remained the same (Fig. 3b). The charge-balanced patterns were as follows: (1) symmetrical cathode-first pulse (Fig. 3ba), (2) asymmetrical large cathode-first pulse (Fig. 3bb), (3) asymmetrical large anode-first pulse (Fig. 3bc), (4) asymmetrical small cathode-first pulse (Fig. 3bd), (5) asymmetrical small anode-first pulse (Fig. 3be).

The inter-pulse duration between cathodic and anodic pulses within each biphasic stimulus was set at 50 μs .

Recordings of cortical evoked potentials

VEPs and EEPs from the visual cortex contralateral to the stimulated eye were recorded by a multi-channel neurophysiology workstation (System 3, Tucker-Davis Technologies, Alachua, FL, USA). Signals from nine recording electrodes were acquired simultaneously at a 6000 Hz sampling rate for each channel, and amplified and filtered with a band-pass of 3 to 2000 Hz. Fifty consecutive evoked responses were averaged and analyzed.

To determine the current threshold for eliciting EEPs at a fixed pulse duration, a sub-threshold current of 10 μA was applied initially, and then the current was increased gradually with steps of 10 μA until reproducible EEPs could be first recorded by one or several electrodes of the recording electrode array. The evoked response was identified only when the first large positive peak (P1) amplitude of EEPs was at least twice the root mean square (RMS) of the baseline fluctuation. To find the lowest stimulating current, the current was then decreased with steps of 5 μA , and then 2.5 μA if necessary, until reproducible EEPs could not be recorded. The lowest current that could elicit EEPs was defined as the current threshold. The charge threshold was calculated by multiplying the current

threshold by the first pulse duration, and the charge density threshold was defined as the charge threshold divided by the exposed area of the electrode tip.

To ensure that EEPs originated from optic nerve stimulation, 1 ml lidocaine (1%) was injected into the optic nerve posterior to the stimulating site to block optic nerve impulses, and the EEP responses prior and posterior to the injection were measured respectively.

Data analysis

Reproducible EEPs could be usually recorded by more than one of the nine electrodes. The maximum of the nine recording responses, which was selected to represent the cortical activities elicited by electrical stimulation of the optic nerve, was analyzed. Therefore, the maximal EEPs recorded by one of the nine electrodes are shown in the figures of this paper, and the P1 amplitude and latency of the maximal EEPs were further analyzed. VEPs were analyzed with the same method. To reduce inter-animal variations, the amplitude of P1 of EEPs was normalized with respect to the maximum amplitude in each animal. The latency of P1 was used because it varied less among animals.

The one-way analysis of variance (one-way ANOVA) [29] was used to determine the significance of modulations in the amplitude of P1 of EEPs when the effects of stimulus waveform were studied. And the paired *t*-test was further applied to analyze the significance of differences in amplitude of P1 elicited by any two of five types of stimulus waveforms. A value of $p < 0.05$ was considered statistically significant.

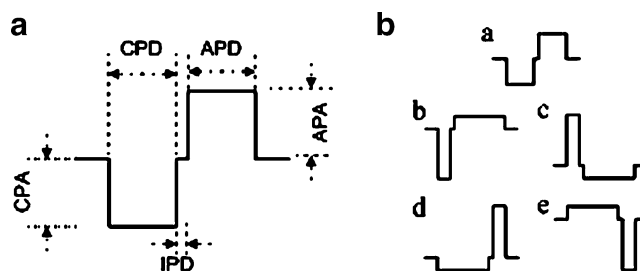


Fig. 3 Diagram of charge-balanced biphasic current pulse. **a** Charge-balanced biphasic pulse. CPA: cathodic pulse amplitude, CPD: cathodic pulse duration, IPD: inter-pulse duration, APA: anodic pulse amplitude, APD: anodic pulse duration. The unit for CPA, APA was μA , for CPD, APD, IPD was ms. **b** Charge-balanced biphasic pulses used in the experiments for evaluating the effects of stimulus waveform: (**ba**) symmetrical cathode-first (CPA: 100, CPD: 0.5, APA: 100, APD: 0.5), (**bb**) asymmetrical large cathode-first (CPA: 200, CPD: 0.25, APA: 50, APD: 1), (**bc**) asymmetrical large anode-first (APA: 200, APD: 0.25, CPA: 50, CPD: 1), (**bd**) asymmetrical small cathode-first (CPA: 50, CPD: 1, APA: 200, APD: 0.25), (**be**) asymmetrical small anode-first (APA: 50, APD: 1, CPA: 200, CPD: 0.25). Inter-pulse duration of all the biphasic pulses was fixed at 50 μs . The symmetrical cathode-first biphasic pulse was used unless specified in this paper

Histological examination

To examine the actual implantation position of the stimulating electrode into the optic nerve, histological analysis was performed on the optic nerve with the electrodes intact after the experiment. Rabbits were euthanized with an overdose of pentobarbital. The eyes were immediately enucleated, and then fixed overnight in 10% neutral formalin solution. After the fixation, the eyes were embedded in paraffin. The electrodes were removed out of the optic nerve before sectioning. Transverse sections of 5 μm in thickness were cut by a wax slice cutting apparatus (RM2135, Leica, Wiesbaden, Germany) and stained with hematoxylin-eosin. The sections were examined by light microscope (SMZ-168, Motic China, Xiamen, China), and the digital images were captured with a CCD color camera (CS5260BDP, Toshiba Teli Co., Tokyo, Japan).

Results

Visually evoked potentials

Before exposing the optic nerve surgically, bright-flash VEPs elicited by white-colored photic stimulus (90 mJ, 1 Hz) were recorded from all of the rabbits ($n=26$). The measured amplitude of P1 was $115.79 \pm 22.97 \mu\text{V}$ (mean \pm SD, the same below) and the latency was $23.28 \pm 1.66 \text{ ms}$. A typical VEP waveform recorded from one of the 26 rabbits is shown in Fig. 4a.

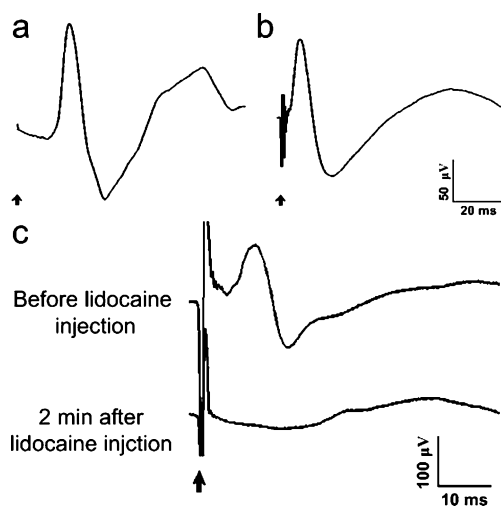


Fig. 4 Typical VEP (a) and EEP (b) waveforms recorded by one epidural recording electrode of the nine-electrode array. These two waveforms were obtained from one rabbit. c EEP waveforms before and after injection of lidocaine into the optic nerve. The waveforms were obtained from another rabbit. The power of visual flash was 90 mJ. The stimulus pulse amplitude was 100 μA and pulse duration was 0.5 ms. Arrows: onset of stimulus

Electrically evoked potentials

Electrical stimulation of the optic nerve induced EEPs in the visual cortex of all the rabbits ($n=26$). The waveform of the induced EEPs was similar to that of VEPs. However, the amplitude of P1 was smaller and the latency of P1 was much shorter than that of VEPs (Fig. 4a,b). The measured amplitude of P1 of EEPs was $92.06 \pm 12.21 \mu\text{V}$ and the latency was $10.79 \pm 2.11 \text{ ms}$ when the optic nerve was stimulated by a charge-balanced biphasic current pulse with 100 μA amplitude and 0.5 ms duration.

After injection of lidocaine into the optic nerve, the EEPs decreased, and no EEPs were recorded 2 min after lidocaine injection (Fig. 4c). As lidocaine blocks the optic nerve impulses, no active signals could be transmitted to the visual cortex via the optic nerve. These results demonstrated that the EEPs recorded in the visual cortex originated from electrical stimulation of the optic nerve.

Threshold for intraorbital optic nerve stimulation

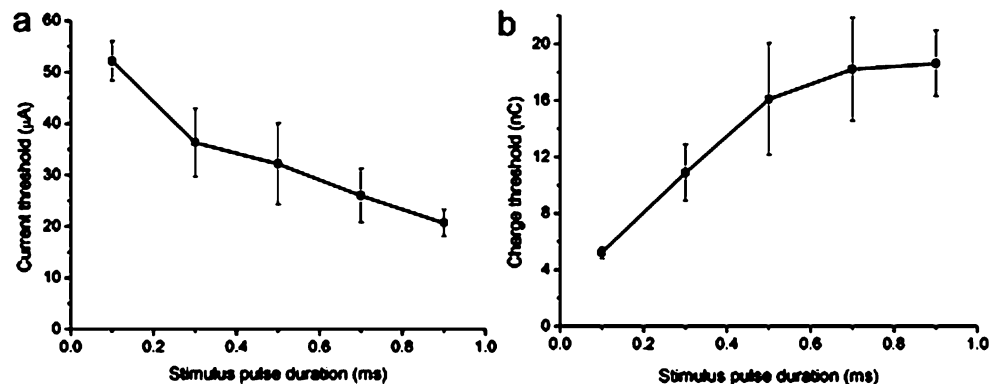
The current threshold for eliciting reproducible EEPs in the visual cortex was $32.63 \pm 8.62 \mu\text{A}$ when the stimulus pulse duration was 0.5 ms ($n=8$). The corresponding charge threshold delivered by the stimulating electrode was $16.32 \pm 4.31 \text{ nC}$. As the exposed surface of the stimulating electrode was approximately $7.64 \times 10^{-4} \text{ cm}^2$, the corresponding charge density threshold was $21.36 \pm 5.64 \mu\text{C}/\text{cm}^2$.

The strength–duration curve was investigated in five rabbits, displayed in Fig. 5a. Current threshold decreased as the pulse duration of the stimulus increased. Figure 5b shows the charge threshold as a function of pulse duration, which was calculated from the data of Fig. 5a. Unlike the current threshold, the corresponding charge threshold increased with increasing pulse duration.

EEPs to stimuli with variable pulse amplitudes

Different cortical responses were elicited when the optic nerve was stimulated by stimuli with variable pulse amplitudes and a fixed pulse duration ($n=5$). Figure 6a depicts the EEP waveforms to stimuli with varying pulse amplitudes. Figure 6b displays the normalized amplitude of P1 as a function of stimulus pulse amplitude. The normalized amplitude of P1 increased from 0.14 ± 0.05 to 1.00 ± 0.00 respectively, as the pulse amplitude increased from 40 to 120 μA (the corresponding charge increased from 20 to 60 nC). Figure 6c shows the changes of latency of P1 with increasing stimulus pulse amplitude. The latency of P1 decreased from $13.21 \pm 1.03 \text{ ms}$ to $10.08 \pm 0.39 \text{ ms}$ with increments of the stimulus pulse amplitude within the range used in the experiments.

Fig. 5 **a** Current threshold as a function of stimulus pulse duration. **b** Corresponding charge threshold as a function of stimulus pulse duration. The charge threshold is calculated by multiplying the stimulus pulse current threshold by the first pulse duration. *Symbols*: means from five rabbits. *Vertical bars*: \pm SD



EEPs to stimuli with variable pulse durations

Different cortical responses were also elicited when the optic nerve was stimulated by stimuli with variable pulse durations and a fixed pulse amplitude ($n=5$). The EEP waveforms to stimuli with varying pulse duration are shown in Fig. 7a. Figure 7b displays the normalized amplitude of P1 as a function of stimulus pulse duration. As can be seen, the normalized amplitude of P1 increased from 0.68 ± 0.07 to 0.99 ± 0.02 respectively, when the pulse duration increased from 0.4 to 1.0 ms. The amplitude of P1 approximately saturated for pulse durations greater than 0.6 ms (the corresponding charge was 60 nC). The latency of P1 changed little with increasing stimulus pulse duration (Fig. 7c).

EEPs to stimuli with fixed charge

The effects of cortical responses to stimuli with fixed charge were explored by stepping up the pulse duration gradually and adjusting the pulse amplitude correspondingly to keep the charge fixed ($n=5$). Figure 8a displays the EEP waveforms elicited by stimuli with an identical charge per pulse, but different pulse amplitude and duration. The waveforms shown in Fig. 8a were recorded when the charge per pulse was fixed at 50 nC. Figure 8b plots the normalized amplitude of P1 as a function of stimulus pulse duration. As depicted in Fig. 8b and c, the normalized amplitude of P1 decreased from 1.00 ± 0.01 to 0.29 ± 0.05 , and the latency increased from 9.37 ± 0.32 to 12.21 ± 1.18 ms, when the pulse duration increased from 0.2

Fig. 6 **a** The EEP waveforms elicited by stimuli with variable pulse amplitudes and a fixed pulse duration. The pulse amplitude ranged from 40 to 120 μ A and the pulse duration was 0.5 ms. The series of waveforms were obtained from one rabbit. *Arrow*: onset of stimulus. Amplitude (**b**) and latency (**c**) of P1 as a function of stimulus pulse amplitude. Amplitude was the normalized value with respect to the maximum. *Symbols*: means from five rabbits. *Vertical bars*: \pm SD

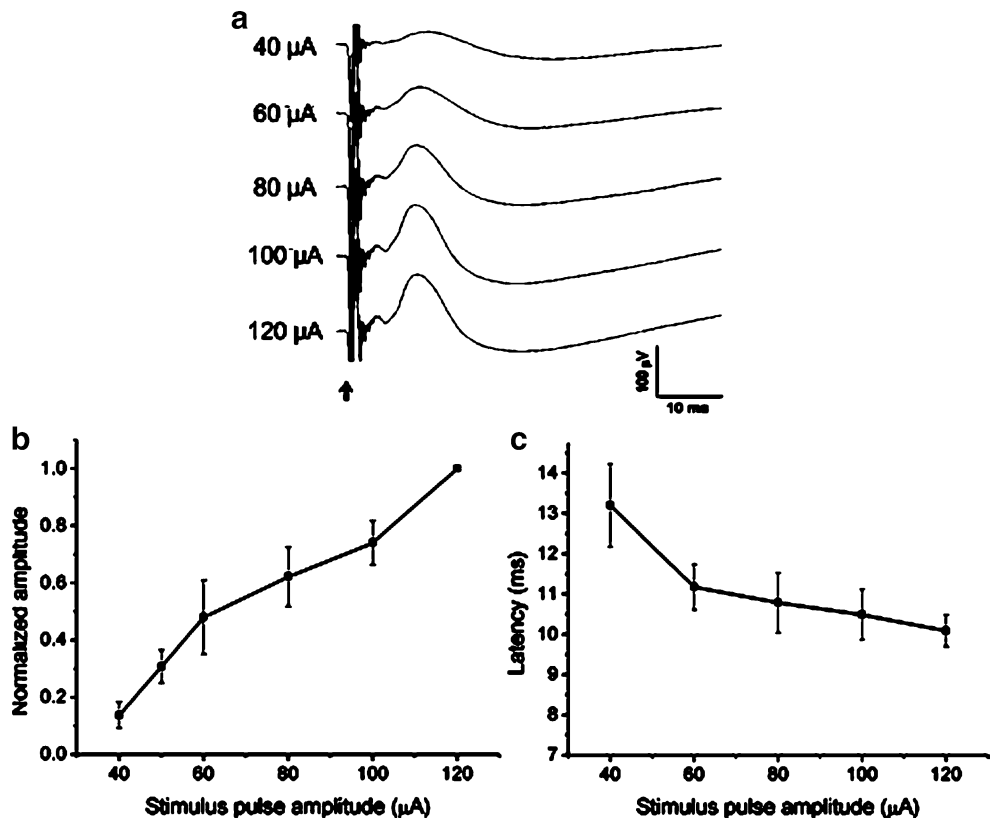


Fig. 7 a The EEP waveforms elicited by stimuli with variable pulse durations and a fixed pulse amplitude. The stimulus pulse duration ranged from 0.4 to 1.2 ms and the pulse amplitude was 100 μ A. The series of waveforms were obtained from one rabbit. *Arrow*: onset of stimulus. Amplitude (**b**) and latency (**c**) of P1 as a function of stimulus pulse duration. Amplitude was the normalized value with respect to the maximum. *Symbols*: means from five rabbits. *Vertical bars*: \pm SD

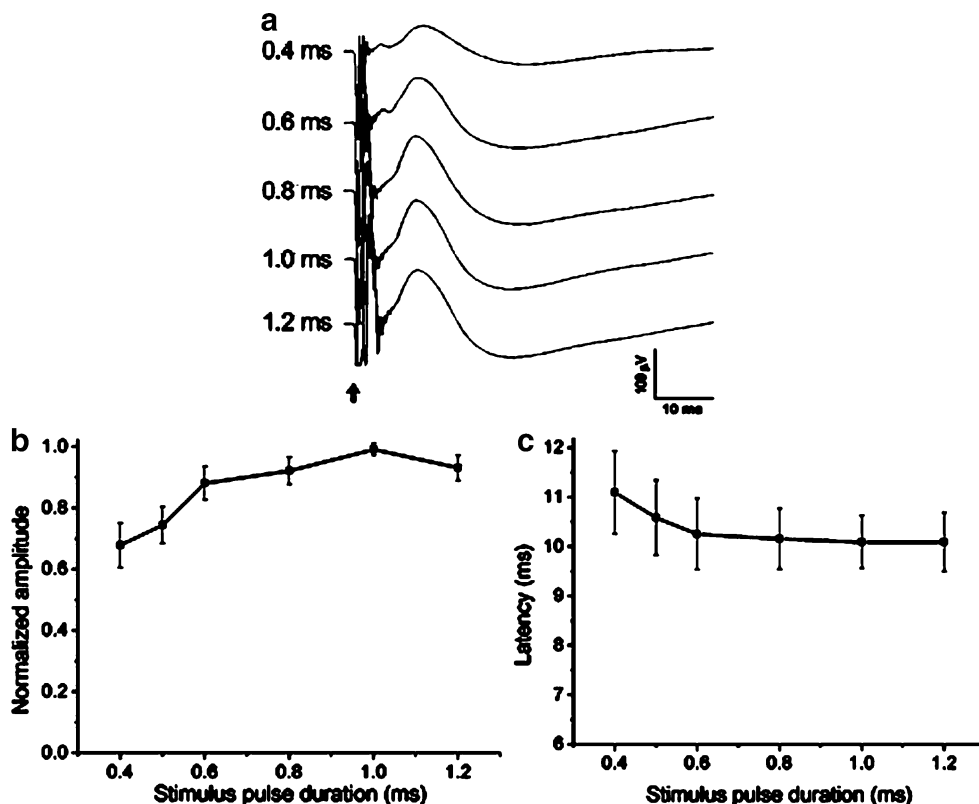
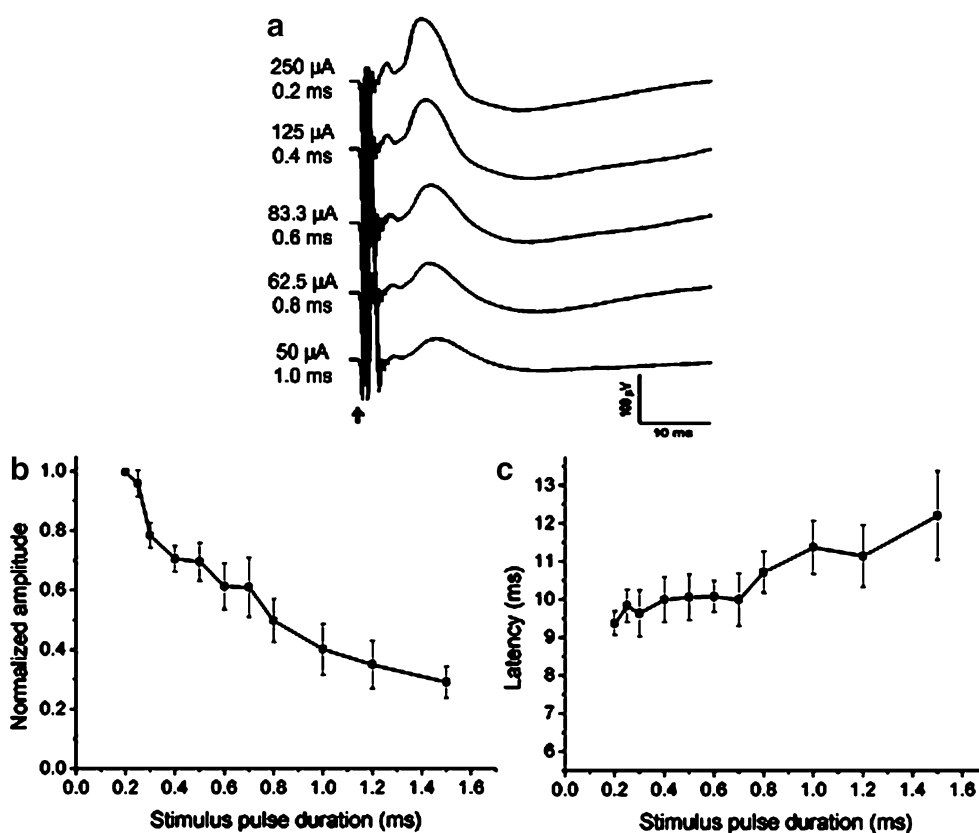


Fig. 8 a The EEP waveforms elicited by stimuli with fixed charge by gradually increasing pulse duration and simultaneously decreasing pulse amplitude. The charge per pulse was 50 nC. The stimulus pulse duration ranged from 0.2 ms to 1.0 ms and the pulse amplitude ranged from 250 to 50 μ A correspondingly. The series of waveforms were obtained from one rabbit. *Arrow*: onset of stimulus. Amplitude (**b**) and latency (**c**) of P1 as a function of stimulus pulse duration with charge fixed at 50 nC. Amplitude was the normalized value with respect to the maximum. *Symbols*: means from five rabbits. *Vertical bars*: \pm SD



1.5 ms (with the pulse amplitude being decreased from 250 to 33.3 μA accordingly). The amplitude of P1 fell by 70.9% and the latency rose by 30.2% when the stimulus pulse duration was increased to 7.5 times of its original length, even though the total charge was fixed.

Effects of stimulus frequency

As the stimulus frequency increased from 1 to 10 Hz, the normalized amplitude of P1 decreased from 1.00 ± 0.00 to 0.31 ± 0.05 (Fig. 9a) and the latency increased from 9.53 ± 0.49 to 12.19 ± 1.27 ms (Fig. 9b) ($n=5$). The mean normalized amplitude of P1 fell to 30.6% of its original value when the stimulus frequency was changed from 1 to 10 Hz. The most significant drop in P1 amplitude (45.7%) occurred when the stimulus frequency was varied from 1 to 2 Hz. The amplitude of P1 then declined more slowly when the stimulus frequency was increased from 2 to 10 Hz.

Effects of stimulus waveform

Five charge-balanced stimulus patterns, all with equal charge (Fig. 3b), were used to investigate the effects of the stimulus waveform on EEPs ($n=5$). The five EEP waveforms displayed in Fig. 10 illustrate the cortical responses elicited by stimuli with different waveforms. The different stimulation artifacts in the EEP recordings correspond with the different stimulus patterns. One-way ANOVA analysis showed a significant difference among amplitudes of P1 elicited by the five different stimulus waveforms ($p < 0.05$, $n=5$). The paired t -test analysis was further made to compare the P1 amplitudes elicited by any two of the five different stimulus waveforms ($n=5$), as shown in Table 1. The symmetrical cathode-first biphasic pulse (Fig. 3ba) evoked the largest P1 amplitude in all of the five rabbits among the five stimulation patterns ($p < 0.05$). The asymmetrical small anode-first biphasic pulse (Fig. 3be) evoked the smallest P1 amplitude among all of the stimulating patterns ($p < 0.05$). The amplitude of P1

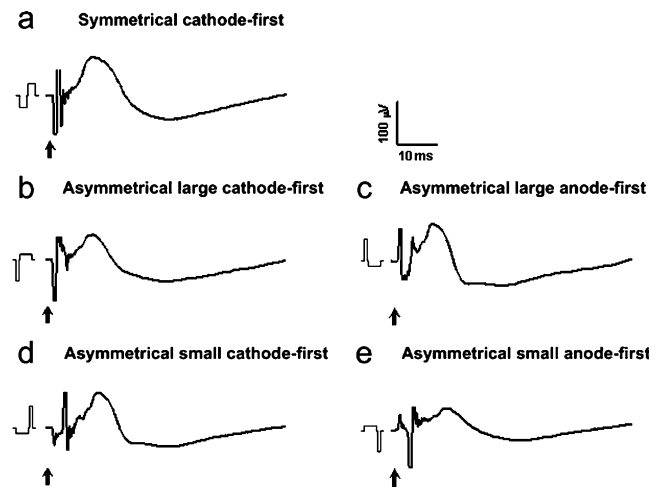


Fig. 10 EEP waveforms elicited by stimuli with different waveforms. The stimulus waveforms are shown anterior to the EEP waveforms. The series of EEP waveforms were obtained from one rabbit. The stimulus waveforms are illustrated in Fig. 3b. Arrows: onset of stimulus

induced by the asymmetrical small anode-first biphasic pulse (Fig. 3be) was very significantly weaker (41.8%) than that evoked by the symmetrical cathode-first biphasic pulse (Fig. 3ba). There was no significant difference among the amplitudes of P1 evoked by asymmetrical large cathode-first biphasic pulse (Fig. 3bb), asymmetrical large anode-first biphasic pulse (Fig. 3bc) and asymmetrical small cathode-first biphasic pulse (Fig. 3bd) ($p > 0.05$, Table 1).

Histology

A photomicrograph of the histological slide of an optic nerve from one untreated eye is shown in Fig. 11a, and that of an optic nerve from one stimulated eye with the stimulating electrode track is shown in Fig. 11b. Histological analysis of transverse sections of the optic nerve of the eyes implanted with electrodes showed that the stimulating electrode was penetrated into the optic nerve, and the depth of the implantation was about 0.5 mm.

Fig. 9 Amplitude (a) and latency (b) of P1 as a function of stimuli with frequency ranging from 1 to 10 Hz. Amplitude was the normalized value with respect to the maximum. The stimulus pulse amplitude was 100 μA and pulse duration was 0.5 ms. Symbols: means from five rabbits. Vertical bars: \pm SD

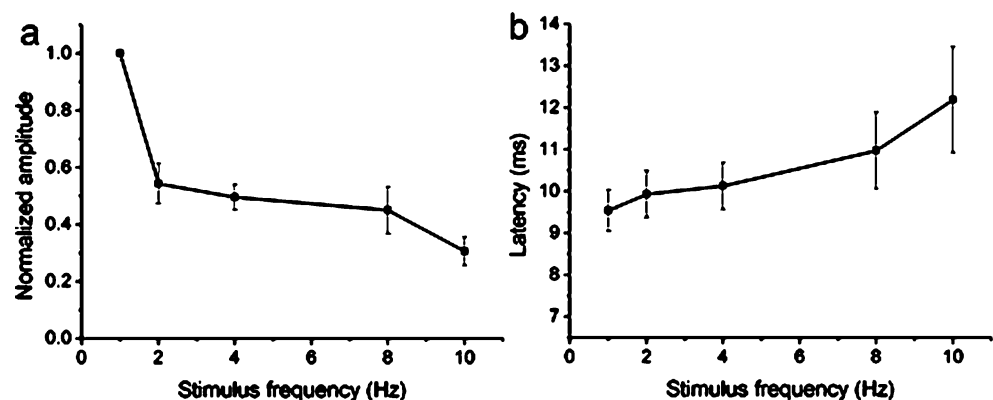


Table 1 Comparisons among the P1 amplitudes of EEPs elicited by five stimulating waveforms using paired *t*-test (*n*=5)

	SCF	ALCF	ALAF	ASCF	ASAF
ALCF	$p < 0.05$				
ALAF	$p < 0.05$	$p = 0.33$			
ASCF	$p < 0.05$	$p = 0.21$	$p = 0.27$		
ASAF	$p < 0.05$	$p < 0.05$	$p < 0.05$	$p < 0.05$	
Mean \pm SD (μ V)	103.51 \pm 8.21	89.44 \pm 6.41	91.86 \pm 4.58	94.95 \pm 6.26	60.23 \pm 15.21

The stimulating waveforms are shown in Fig. 3b. SCF: symmetrical cathode-first (Fig. 3ba); ALCF: asymmetrical large cathode-first (Fig. 3bb); ALAF: asymmetrical large anode-first (Fig. 3bc); ASCF: asymmetrical small cathode-first (Fig. 3bd); ASAF: asymmetrical small anode-first (Fig. 3be). The row of Mean \pm SD shows average and standard deviation of P1 amplitude of EEPs elicited by stimulating waveforms SCF, ALCF, ALAF, ASCF and ASAF respectively.

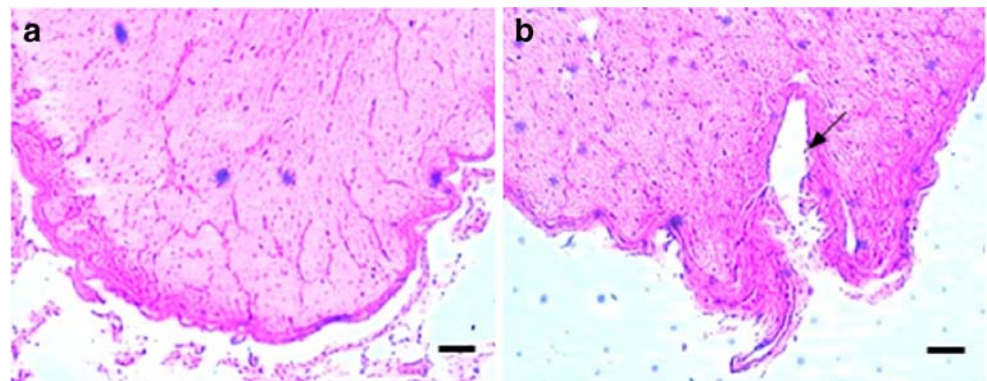
Discussion

Visual prostheses based on optic nerve stimulation represent an alternative to those which involve direct retinal stimulation. Several other studies have investigated visual prostheses based on optic nerve stimulation. Veraart et al. reported different phosphenes could be evoked by electrical stimulation of the optic nerve with surface electrodes in humans [41, 42]. Sakaguchi et al. and Fang et al. stimulated the optic nerve head intraocularly with implanted penetrating electrodes in rabbits. Their results demonstrated that cortical responses could be elicited by this approach [8, 9, 38]. However, the optimal stimulus parameters to activate the optic nerve have not been investigated systematically. Our present study provides critical experimental data that could be used to design sensible stimulating protocols for visual prosthesis based on penetrative optic nerve stimulation.

In our experiment, visual cortex responses were successfully evoked by intraorbital optic nerve stimulation with penetrating electrodes in rabbits. The EEP waveforms were similar to the VEP waveforms. Compared with VEPs, the shortened latency of P1 of EEPs is presumably due to the fact that the direct electrical stimulation of axons of ganglion cells spares the time that is needed for processing visual inputs by retinal cells. With single biphasic rectangular pulse stimulation, the charge density threshold in our study was $21.36 \pm 5.64 \mu\text{C}/\text{cm}^2$, while $6.21 \mu\text{C}/\text{cm}^2$ was

obtained in rabbits by stimulating the optic nerve head [9] and $80 \mu\text{C}/\text{cm}^2$ was obtained in a blind patient (calculated at pulse duration of $404.7 \mu\text{s}$) with surface cuff electrodes around the optic nerve [5]. These results suggest that optic nerve stimulation with penetrating electrodes can have much lower thresholds than that with surface electrodes. Compared with our data, the lower threshold of stimulating the optic nerve head reported by Fang et al. [9] was probably due to the difference in the material and the exposed surface of stimulating electrodes. In their study, platinum wire was used as stimulating electrode, and the exposed surface of stimulating electrode was about $0.4 \times 10^{-4} \text{cm}^2$ larger than ours. In vivo retinal electrical stimulation experiments were also performed by several research groups in the rabbits. For subretinal stimulation, Gekeler et al. obtained an average charge density threshold of $50 \mu\text{C}/\text{cm}^2$ [49] and that of Schwahn et al.'s study was about $70 \mu\text{C}/\text{cm}^2$ [50]. For epiretinal stimulation, Humayun et al. obtained a charge density threshold of $8.92 \mu\text{C}/\text{cm}^2$ for normal rabbits and $11.9 \mu\text{C}/\text{cm}^2$ for rabbit retinas with outer retinal degenerations [51]. Epiretinal stimulating charge density threshold in rabbits by Walter et al. was $1 \sim 12 \mu\text{C}/\text{cm}^2$ [43]. Compared with these data, the threshold obtained by the present study is comparable with that by epiretinal stimulation and much lower than that by subretinal stimulation. The nerve fiber layer and/or the ganglion cell layer are considered to be stimulated

Fig. 11 Light photomicrographs of transverse sections of optic nerves for comparison. **a** A slice of the optic nerve from an untreated eye. **b** A slice from a stimulated eye with the track of the penetrating electrode (labeled with *arrow*). The depth of the insertion of the electrode into the optic nerve was about $500 \mu\text{m}$. Scale bars: $100 \mu\text{m}$



preferentially in the epiretinal approach. The optic nerve fibers are stimulated in our study; therefore, the threshold obtained by present study is at a similar level to that by epiretinal stimulation. In the subretinal approach, photoreceptors and/or the bipolar cells are thought to be the main target neurons of the electrical stimulation. The threshold difference between the epiretinal and subretinal approaches may be due to the morphological differences of the target neurons in these two approaches. The higher threshold of the subretinal stimulation may also be related to the edema of the retina caused by the subretinal surgery [49]. However, Chow et al. showed a threshold charge density of 2.8 nC/cm^2 [3], which is much lower than the data above. The much lower threshold is probably due to the huge surface area of the stimulating electrode (36 mm^2), which may be not appropriate for clinical use due to its big size and low spatial resolution.

The stimulating charge and its dynamic range are important parameters in designing visual prostheses. From the results of EEPs to variable stimulus pulse amplitudes and durations in our study (Figs. 6b and 7b), we note that the amplitude of P1 increased linearly with increments of the stimulus charge up to around 60 nC, at which stage saturation occurred. Therefore, the dynamic range in our experiments with intraorbital optic nerve stimulation was about 0.48 log units (20 to 60 nC). The dynamic range in Gekeler et al.'s study for subretinal stimulation was from 0.1 to 1.3 log units [49] and that in Humayun et al.'s study for epiretinal stimulation which could elicit phosphenes with different brightness was from 0.48 to 0.94 log units [52]. These data are at a similar level to ours, which suggests that phosphenes with different brightness might be activated by intraorbital optic nerve stimulation within a similar dynamic charge range with retinal stimulation. It has been reported that charge and charge density are important factors in inducing neural damage [28]. An empirical equation based on the relationship of charge and charge density was derived for the maximum safe level for electrical stimulation [40]. Based on this empirical equation, the safe charge level for neural stimulation with the exposed area of the penetrating electrode ($7.64 \times 10^{-4} \text{ cm}^2$) should be below 155 nC. Therefore, stimulus charges within the range of 20–60 nC may be suitable and safe for eliciting cortical responses by optic nerve stimulation with our penetrating electrodes.

The duration of the stimulating pulses is another important factor to be considered in visual prosthesis design. As illustrated in Fig. 8, the amplitude of P1 decreased and the latency of P1 increased as the stimulus pulse duration increased from 0.2 to 1.5 ms with stimulus charge fixed. The stimulus with a shorter pulse duration induced a larger amplitude P1 than that with a longer pulse duration. This finding agrees with the results obtained from

the charge-duration curves shown in Fig. 5b, which demonstrated that the charge threshold increased with the increment of the stimulus pulse duration. Our experimental results indicate that stimuli with shorter pulse durations are more efficacious for eliciting EEPs than those with longer pulse durations, and stimuli with shorter pulse durations should be applied to stimulate the optic nerve to minimize the total charge injected into the neural tissue. These findings are in agreement with similar studies based on direct retinal stimulation. Jensen et al. [19] examined the effects of stimulus pulse duration on the current and charge threshold for stimulation of the rabbit retinal ganglion cells in vitro. Their results showed that the current threshold for activation of retinal ganglion cells decreased and the charge threshold increased as stimulus pulse duration increased from 0.1 to 50 ms. Rizzo III et al. [34] performed epiretinal electrical stimulation in humans, and discovered a similar phenomenon, that current threshold increased and charge threshold decreased with shorter stimulus pulse duration.

In our study, we found that the P1 amplitude of EEPs declined as the stimulus frequency was increased from 1 to 10 Hz (Fig. 9a). Similar results were reported by Foerster et al. [10] in visual stimulation of the retina with different flash frequencies in human. Direct electrical stimulation of the retina also induced a decrease in the cortical evoked responses when the stimulus frequency increased from 0.5 to 16 Hz [31]. Compared with the results of retina stimulation, our data showed that the depression of EEPs was more pronounced at lower frequencies (1–2 Hz). The discrepancies may arise from activation of different parts of the visual system. Nevertheless, these results support the finding that ganglion cell responses to a stimulation pulse applied after a preceding one were depressed when the interval between the two pulses decreased [17]. In addition, McCreedy et al. [27] found that continuous low frequency stimulation of cat's sciatic nerve induced little neural injury, even when the stimulus amplitude was high. The finding indicates that low frequency stimulation of the optic nerve may alleviate neural damage to the optic nerve, although the assessment should be carried out in the future. Herein, stimuli with low frequency are suggested to be preferable ones to stimulate the optic nerve directly.

An interesting finding was the influence of stimulus waveform on EEPs. Among the five charge-balanced stimulus waveforms with the same charge used in this study, symmetrical cathode-first biphasic pulse (Fig. 3ba) yielded the largest cortical potentials, while asymmetrical small anode-first biphasic pulse (Fig. 3be) yielded the smallest ones (Fig. 10, Table 1). Our results were different from the findings for retina stimulation. Rizzo III et al. [31] found that large cathode-first pulse was most effective among the asymmetrical pulses to evoke cortical responses. However, in our study, the asymmetrical large cathode-first

pulse (Fig. 3bb) didn't evoke EEP responses significantly different to those obtained with the asymmetrical large anode-first biphasic pulse (Fig. 3bc) and the asymmetrical small cathode-first biphasic pulse (Fig. 3bd), although the asymmetrical large cathode-first pulse (Fig. 3bb) evoked significantly larger EEPs than the asymmetrical small anode-first biphasic pulse (Fig. 3be, Table 1). The differences may result from two reasons: firstly, bipolar stimulation mode was used in our study, while monopolar stimulation mode (with a return electrode on the ear) was used in their study. Secondly, in our experiments only the optic nerve was electrically stimulated while they probably stimulated the nerve fiber layer and the ganglion cell layer simultaneously. Our results from other experiments showed that the cortical potentials evoked by symmetrical anode-first biphasic pulse were smaller than the ones evoked by symmetrical cathode-first biphasic pulse. Therefore, symmetrical anode-first biphasic pulses were not used in this study. As symmetrical cathode-first biphasic pulses yielded the largest potentials among the charge-balanced patterns with the same charge, our experimental results indicate that symmetrical cathode-first biphasic pulses are a more appropriate way to stimulate the optic nerve directly. Grill et al. [11] demonstrated that selective stimulation of nerve fibers could be achieved by selecting stimulus waveforms. The short-duration stimuli could activate large diameter fibers before small fibers by modulating the opening and closing of m and h gates of the fiber membrane. The influence of stimulus waveform on EEPs by optic nerve stimulation observed in this study may be related to the selective activation of different optic nerve fibers. Further investigation should be performed to elucidate the mechanisms underlying the effects of stimulating waveforms on EEPs in the future study.

For VEP evaluation during the entire experiments, the amplitude of P1 of VEPs decreased immediately after surgical exposure of the optic nerve compared with that recorded prior to surgery. However, the amplitude of P1 did not vary significantly after the insertion of the stimulating electrodes into the optic nerve and during the entire stimulating procedure, which suggested that no obvious damage to the visual function was introduced by insertion of the stimulating electrodes and electrical stimulation in acute experiments. The results revealed that in the acute experiment, the orbital surgery may cause some unwanted manipulations of the optic nerve, which in turn may lead to some adverse effect on the visual system of the animal. This suggests that the surgical procedure for our experiments could be improved to minimize unwanted surgical manipulation to the optic nerve. Further investigation of the surgical procedure is underway using minimally invasive endoscopic techniques for the implantation of the micro-electrode array.

The acute electrophysiological study provides useful information on the optimal parameters and dynamic range of the optic nerve stimulation. However, the threshold and response properties may change after long-term implantation of the stimulating electrodes into the optic nerve, which results from the displacement of the electrodes, tissue damage induced by the electrode implantation and electrical stimulation, and encapsulation of the electrodes. Thus, a long-term evaluation of the optic nerve stimulation should be performed in a future study.

The advantages of the visual prosthesis based on optic nerve stimulation include possible coverage of the whole visual field, not requiring intraocular surgery and not disturbing retinal tissues; however, this approach still needs to overcome many obstacles, including selective stimulation of optic nerve fibers with limited number of electrodes, reducing the optic nerve damage caused by implantation of electrodes, and so on.

In conclusion, our study demonstrates that intraorbital optic nerve stimulation by penetrating electrodes can evoke visual cortical responses with low charge density thresholds. Response properties of EEPs suggest that short-duration symmetrical cathode-first biphasic pulses of current with low frequencies are more efficacious in eliciting electrophysiological responses at visual cortex than other stimulation waveforms. Further investigations are underway, including improvement of surgical techniques, stimulation selectivity with reduced electrode size in an array, intraorbital optic nerve stimulation in other animal models, and long-term evaluation of this approach.

Acknowledgements The authors thank Yuxiu Liu and Xiaoliang Li for performing the animal surgery; Xiaohong Sui for providing technical supports on electrode fabrication; Niall McLoughlin for providing valuable reviews and comments on the manuscript.

This research is supported by the National Basic Research Program of China (973 Program, 2005CB724302), National Science Fund for Distinguished Young Scholars from The National Natural Science Foundation of China (60588101), Shanghai Pujiang Program (07pj14050), Shanghai Commission of Science and Technology (05DZ22318, 05DZ22325, 04DZ05114).

References

1. Branner A, Normann RA (2000) A multielectrode array for intrafascicular recording and stimulation in sciatic nerve of cats. *Brain Res Bull* 51:293–306, doi:10.1016/S0361-9230(99)00231-2
2. Branner A, Stein RB, Normann RA (2001) Selective stimulation of cat sciatic nerve using an array of varying-length micro-electrodes. *J Neurophysiol* 85:1585–1594
3. Chow AY, Chow VY (1997) Subretinal electrical stimulation of the rabbit retina. *Neurosci Lett* 225:13–16, doi:10.1016/S0304-3940(97)00185-7
4. Chow AY, Chow VY, Packo KH, Pollack JS, Peyman GA, Schuchard R (2004) The artificial silicon retina microchip for the

- treatment of vision loss from retinitis pigmentosa. *Arch Ophthalmol* 122:460–469, doi:10.1001/archophth.122.4.460
5. Delbeke J, Wanet-Defalque MC, Gerard B, Troosters M, Michaux G, Veraart C (2002) The microsystems based visual prosthesis for optic nerve stimulation. *Artif Organs* 26:232–234, doi:10.1046/j.1525-1594.2002.06939.x
 6. DeMarco PJ Jr, Yarbrough GL, Yee CW, McLean GY, Sagdullaev BT, Ball SL et al (2007) Stimulation via a subretinally placed prosthetic elicits central activity and induces a trophic effect on visual responses. *Invest Ophthalmol Vis Sci* 48:916–926, doi:10.1167/iovs.06-0811
 7. Eckmuller R (1997) Learning retina implants with epiretinal contacts. *Ophthalmic Res* 29:281–289
 8. Fang X, Sakaguchi H, Fujikado T, Osanai M, Ikuno Y, Kamei M et al (2006) Electrophysiological and histological studies of chronically implanted intrapapillary microelectrodes in rabbit eyes. *Graefes Arch Clin Exp Ophthalmol* 244:364–375, doi:10.1007/s00417-005-0073-9
 9. Fang X, Sakaguchi H, Fujikado T, Osanai M, Kanda H, Ikuno Y et al (2005) Direct stimulation of optic nerve by electrodes implanted in optic disc of rabbit eyes. *Graefes Arch Clin Exp Ophthalmol* 243:49–56, doi:10.1007/s00417-004-0957-0
 10. Foerster M, Li X (1986) Evaluation of the central retina and optic nerve function in media opacities. *Doc Ophthalmol* 63:101–106, doi:10.1007/BF00153017
 11. Grill WM, Mortimer JT (1995) Stimulus waveforms for selective neural stimulation. *IEEE Eng Med Biol Mag* 14:375–385, doi:10.1109/51.395310
 12. Heckenlively JR, Boughman J, Friedman L (1988) Diagnosis and classification of retinitis pigmentosa. Lippincott, Philadelphia
 13. Hornig R, Laube T, Walter P, Velikay-Parel M, Bornfeld N, Feucht M, Akguel H, Rössler G, Altheheld N, Notarp DL, Wyatt J, Richard G (2005) A method and technical equipment for an acute human trial to evaluate retinal implant technology. *J Neural Eng* 2: S129–S134, doi:10.1088/1741-2560/2/1/014
 14. Humayun M (1997) Electrical stimulation of the retina in patients with photoreceptor loss. *Invest Ophthalmol Vis Sci* 38:S39
 15. Humayun MS, De Juan E Jr, Weiland JD, Dagnelie G, Katona S, Greenberg R et al (1999) Pattern electrical stimulation of the human retina. *Vision Res* 39:2569–2576, doi:10.1016/S0042-6989(99)00052-8
 16. Humayun MS, Prince M, De Juan E Jr, Barron Y, Moskowitz M, Klock IB et al (1999) Morphometric analysis of the extramacular retina from postmortem eyes with retinitis pigmentosa. *Invest Ophthalmol Vis Sci* 40:143–148
 17. Jensen RJ, Rizzo JF III (2007) Responses of ganglion cells to repetitive electrical stimulation of the retina. *J Neural Eng* 4:S1–S6, doi:10.1088/1741-2560/4/1/S01
 18. Jensen RJ, Ziv OR, Rizzo JF III (2005) Responses of rabbit retinal ganglion cells to electrical stimulation with an epiretinal electrode. *J Neural Eng* 2:S16–S21, doi:10.1088/1741-2560/2/1/003
 19. Jensen RJ, Ziv OR, Rizzo JF III (2005) Thresholds for activation of rabbit retinal ganglion cells with relatively large, extracellular microelectrodes. *Invest Ophthalmol Vis Sci* 46:1486–1496, doi:10.1167/iovs.04-1018
 20. Kanda H, Morimoto T, Fujikado T, Tano Y, Fukuda Y, Sawai H (2004) Electrophysiological studies of the feasibility of supra-choroidal-transretinal stimulation for artificial vision in normal and RCS rats. *Invest Ophthalmol Vis Sci* 45:560–566, doi:10.1167/iovs.02-1268
 21. Kim SY, Sadda S, Humayun MS, De Juan E Jr, Melia BM, Green WR (2002) Morphometric analysis of the macula in eyes with geographic atrophy due to age-related macular degeneration. *Retina* 22:464–470, doi:10.1097/00006982-200208000-00011
 22. Kim SY, Sadda S, Pearlman J, Humayun MS, De Juan E Jr, Melia BM et al (2002) Morphometric analysis of the macula in eyes with disciform age-related macular degeneration. *Retina* 22:471–477, doi:10.1097/00006982-200208000-00012
 23. Klein R, Klein BEK, Linton KLP (1992) Prevalence of age-related maculopathy: The Beaver Dam Eye Study. *Ophthalmology* 99:933–943
 24. Li L, Hayashida Y, Yagi T (2005) Temporal properties of retinal ganglion cell responses to local transretinal current stimuli in the frog retina. *Vision Res* 45:263–273, doi:10.1016/j.visres.2004.08.002
 25. Margalit E, Maia M, Weiland JD, Greenberg RJ, Fujii GY, Torres G, Priyathaisere DV, O’Hearn TD, Liu W, Lazzi G, Dagnelie G, Scribner DA, Juan ED, Humayun MS (2002) Retinal prosthesis for the blind. *Surv Ophthalmol* 47:335–356, doi:10.1016/S0039-6257(02)00311-9
 26. Maynard EM (2001) Visual prostheses. *Ann Biomed Eng* 3:145–168, doi:10.1146/annurev.bioeng.3.1.145
 27. McCreery D, Agnew W, Yuen T, Bullara L (1995) Relationship between stimulus amplitude, stimulus frequency and neural damage during electrical stimulation of sciatic nerve of cat. *Med Biol Eng Comput* 33:426–429, doi:10.1007/BF02510526
 28. McCreery DB, Agnew WF, Yuen TGH, Bullara L (1990) Charge density and charge per phase as cofactors in neural injury induced by electrical stimulation. *IEEE Trans Biomed Eng* 37:996–1001, doi:10.1109/10.102812
 29. Miller RG (1997) Beyond ANOVA: Basics of Applied Statistics. Chapman & Hall, Boca Raton, FL
 30. Ren QS, Chai XY, Wu KJ, Zhou CQ (2007) Development of C-Sight Visual Prosthesis Based on Optical Nerve Stimulation with Penetrating Electrode Array. *Invest Ophthalmol Vis Sci* 48:661, doi:10.1167/iovs.06-0717
 31. Rizzo JF III, Goldbaum S, Shahin M, Denison TJ, Wyatt J (2004) In vivo electrical stimulation of rabbit retina with a micro-fabricated array: Strategies to maximize responses for prospective assessment of stimulus efficacy and biocompatibility. *Restor Neurol Neurosci* 22:429–443
 32. Rizzo JF III, Wyatt J (1997) Prospects for a visual prosthesis. *Neuroscientist* 3:251–262, doi:10.1177/107385849700300413
 33. Rizzo JF III, Wyatt J, Humayun M, De Juan E, Liu W, Chow A et al (2001) Retinal prosthesis: an encouraging first decade with major challenges ahead: editorial. *Ophthalmology* 108:13–14, doi:10.1016/S0161-6420(00)00430-9
 34. Rizzo JF III, Wyatt J, Loewenstein J, Kelly S, Shire D (2003) Methods and perceptual thresholds for short-term electrical stimulation of human retina with microelectrode arrays. *Invest Ophthalmol Vis Sci* 44:5355–5361, doi:10.1167/iovs.02-0819
 35. Rizzo JF III, Wyatt J, Loewenstein J, Kelly S, Shire D (2003) Perceptual efficacy of electrical stimulation of human retina with a microelectrode array during short-term surgical trials. *Invest Ophthalmol Vis Sci* 44:5362–5369, doi:10.1167/iovs.02-0817
 36. Rosahl SK, Mark G, Herzog M, Pantazis C, Gharabaghi F, Matthies C et al (2001) Far-field responses to stimulation of the cochlear nucleus by microsurgically placed penetrating and surface electrodes in the cat. *J Neurosurg* 95:845–852
 37. Sachs HG, Schanze T, Wilms M, Rentzos A, Brunner U, Gekeler F et al (2005) Subretinal implantation and testing of polyimide film electrodes in cats. *Graefes Arch Clin Exp Ophthalmol* 243:464–468, doi:10.1007/s00417-004-1049-x
 38. Sakaguchi H, Fujikado T, Kanda H, Osanai M, Fang X, Nakauchi K et al (2004) Electrical stimulation with a needle-type electrode inserted into the optic nerve in rabbit eyes. *Jpn J Ophthalmol* 48:552–557, doi:10.1007/s10384-004-0114-7
 39. Santos A, Humayun MS, De Juan E Jr, Greenburg RJ, Marsh MJ, Klock IB et al (1997) Preservation of the inner retina in retinitis pigmentosa: a morphometric analysis. *Arch Ophthalmol* 115:511–515
 40. Shannon RV (1992) A model of safe levels for electrical stimulation. *IEEE Trans Biomed Eng* 39:424–426, doi:10.1109/10.126616

41. Veraart C, Raftopoulos C, Mortimer JT, Delbeke J, Pins D, Michaux G et al (1998) Visual sensations produced by optic nerve stimulation using an implanted self-sizing spiral cuff electrode. *Brain Res* 813:181–186, doi:[10.1016/S0006-8993\(98\)00977-9](https://doi.org/10.1016/S0006-8993(98)00977-9)
42. Veraart C, Wanet-Defalque MC, Gérard B, Vanlierde A, Delbeke J (2003) Pattern recognition with the optic nerve visual prosthesis. *Artif Organs* 27:996–1004, doi:[10.1046/j.1525-1594.2003.07305.x](https://doi.org/10.1046/j.1525-1594.2003.07305.x)
43. Walter P, Heimann K (2000) Evoked cortical potentials after electrical stimulation of the inner retina in rabbits. *Graefes Arch Clin Exp Ophthalmol* 238:315–318, doi:[10.1007/s004170050358](https://doi.org/10.1007/s004170050358)
44. Walter P, Kisvárdy ZF, Görtz M, Alteheld N, Rossler G, Stieglitz T, Eysel UT (2005) Cortical activation via an implanted wireless retinal prosthesis. *Invest Ophthalmol Vis Sci* 46:1780–1785, doi:[10.1167/iovs.04-0924](https://doi.org/10.1167/iovs.04-0924)
45. Weiland JD, Liu W, Humayun MS (2005) Retinal prosthesis. *Ann Biomed Eng* 7:361–401, doi:[10.1146/annurev.bioeng.7.060804.100435](https://doi.org/10.1146/annurev.bioeng.7.060804.100435)
46. Zrenner E (2002) Will retinal implants restore vision? *Science* 295:1022–1025, doi:[10.1126/science.1067996](https://doi.org/10.1126/science.1067996)
47. Zrenner E, Miliczek KD, Gabel VP, Graf HG, Guenther E, Haemmerle H et al (1997) The development of subretinal microphotodiodes for replacement of degenerated photoreceptors. *Ophthalmic Res* 29:269–280
48. Zrenner E, Stett A, Weiss S, Aramant RB, Guenther E, Kohler K et al (1999) Can subretinal microphotodiodes successfully replace degenerated photoreceptors. *Vision Res* 39:2555–2567, doi:[10.1016/S0042-6989\(98\)00312-5](https://doi.org/10.1016/S0042-6989(98)00312-5)
49. Gekeler F, Kobuch K, Schwahn HN, Stett A, Shinoda K, Zrenner E (2004) Subretinal electrical stimulation of the rabbit retina with acutely implanted electrode arrays. *Graefes Arch Clin Exp Ophthalmol* 242:587–596, doi:[10.1007/s00417-004-0862-6](https://doi.org/10.1007/s00417-004-0862-6)
50. Schwahn HN, Gekeler F, Kohler K, Kobuch K, Sachs HG, Schulmeyer F et al (2001) Studies on the feasibility of a subretinal visual prosthesis: data from Yucatan micropig and rabbit. *Graefes Arch Clin Exp Ophthalmol* 239:961–967, doi:[10.1007/s004170100368](https://doi.org/10.1007/s004170100368)
51. Humayun MS, Propst RH, de Juan EJ, McCormick K, Hickingbotham D (1994) Bipolar surface electrical stimulation of the vertebrate retina. *Arch Ophthalmol* 112:110–116
52. Humayun MS, Weiland JD, Fujii GY, Greenberg R, Williamson R, Little J, Mechb B, Cimmarrustib V, Boemela GV, Dagneliec G, Juan E de Jr (2003) Visual perception in a blind subject with a chronic microelectronic retinal prosthesis. *Vision Res* 43:2573–2581, doi:[10.1016/S0042-6989\(03\)00457-7](https://doi.org/10.1016/S0042-6989(03)00457-7)